AMMRC TR 79-54

AD

AD A079563

LEVEL II

SCATTERED LIGHT PHOTOELASTIC ANALYSIS OF A PROJECTILE BULKHEAD TO STRUCTURAL CASE JOINT

MILOSLAV BENICEK and JIRO ADACHI
ENGINEERING MECHANICS DIVISION

DDC
RECEIVED
JAN 18 1980
A

DDC FILE COPY

October 1979

Approved for public release; distribution unlimited.

ARMY MATERIALS AND MECHANICS RESEARCH CENTER
Watertown, Massachusetts 02172

80 1 18 009

The findings in this report are not to be construed as an official Department of the Army position, unless so designated by other authorized documents.

Mention of any trade names or manufacturers in this report shall not be construed as advertising nor as an official indorsement or approval of such products or companies by the United States Government.

DISPOSITION INSTRUCTIONS

Destroy this report when it is no longer needed.
Do not return it to the originator.

UNCLASSIFIED

SECURITY CLASSIFICATION OF THIS PAGE (When Data Entered)

REPORT DOCUMENTATION PAGE	READ INSTRUCTIONS BEFORE COMPLETING FORM
1. REPORT NUMBER: AMMRC-TR-79-54 (14)	2. GOVT ACCESSION NO.
3. RECIPIENT'S CATALOG NUMBER	
4. TITLE (and Subtitle): SCATTERED LIGHT PHOTOELASTIC ANALYSIS OF A PROJECTILE BULKHEAD TO STRUCTURAL CASE JOINT. (6)	5. TYPE OF REPORT & PERIOD COVERED: Final Report (9)
	6. PERFORMING ORG. REPORT NUMBER
7. AUTHOR(s): Miloslav Benicek [redacted] Jiro Adachi (10)	8. CONTRACT OR GRANT NUMBER(s) (16)
9. PERFORMING ORGANIZATION NAME AND ADDRESS: Army Materials and Mechanics Research Center, Watertown, Massachusetts 02172, DRXMR-TE	10. PROGRAM ELEMENT, PROJECT, TASK AREA & WORK UNIT NUMBERS: D/A Project: 1X464603D663; AMCMS Code: 36525000204; Agency Accession: DA OF4767
11. CONTROLLING OFFICE NAME AND ADDRESS: U. S. Army Materiel Development and Readiness Command, Alexandria, Virginia 22333	12. REPORT DATE: (11) Oct [redacted] 79; 13. NUMBER OF PAGES: 15
14. MONITORING AGENCY NAME & ADDRESS(if different from Controlling Office) (12) 19	15. SECURITY CLASS. (of this report): Unclassified; 15a. DECLASSIFICATION/DOWNGRADING SCHEDULE

16. DISTRIBUTION STATEMENT (of this Report)

Approved for public release; distribution unlimited.

17. DISTRIBUTION STATEMENT (of the abstract entered in Block 20, if different from Report)

18. SUPPLEMENTARY NOTES

19. KEY WORDS (Continue on reverse side if necessary and identify by block number)

Stress analysis
Photoelasticity
Projectiles
Pin joints
Stress concentration

20. ABSTRACT (Continue on reverse side if necessary and identify by block number)

(SEE REVERSE SIDE)

DD FORM 1 JAN 73 1473 EDITION OF 1 NOV 65 IS OBSOLETE

UNCLASSIFIED 403 105

SECURITY CLASSIFICATION OF THIS PAGE (When Data Entered)

Block No. 20

ABSTRACT

Photoelastic stress analysis of the bulkhead-to-structural case pin joint of a projectile was carried out using the scattered light technique. Analysis provided three-dimensional stress distributions in critical areas of the joint including the pinhole, pin bearing surfaces, and joint bearing surfaces. Stress gradients through the wall were found to be large; however, stress concentrations were found to be moderate with a maximum value of 3.7.

CONTENTS

Accession For
NTIS GRA&I
DDC TAB
Unannounced
Justification
By
Distribution/
Availability Codes
Dist | Avail and/or special
A

I. INTRODUCTION

In advanced artillery shells, the most severe stresses and stress concentrations are encountered in the pins, pinholes, or at the fillets of the joints. There is always concern that failure will start in these areas.

Since practical and accurate mathematical three-dimensional analysis of the pin, the pinhole area, and the joint is beyond the present state-of-the-art, it is necessary to use other means to predict stress values when the need arises. For this reason a photoelastic stress analysis of the rear joint of a recent projectile was undertaken to examine the stress conditions throughout the joint, particularly at contact areas of the pin and pinhole walls and on the mating surfaces of the joint where high stress gradients and stress concentrations were expected to arise.

The scattered light technique of photoelasticity was used for this investigation. With this technique stress variations throughout the specimen thickness can be determined in three dimensions without slicing the model, allowing the possibility for studying the effect of different pin interference values on the stresses merely by change of pins and/or pin interference.

II. EXPERIMENTAL PROCEDURE

A. Frozen Stress Model Preparation

The rear joint has an outside diameter of 8 inches and inside diameter of 7.6 inches. There are sixteen pins equally spaced around the circumference. To simplify the analysis a segment representing one-sixteenth of the periphery with the pin centrally located was modeled, see Figure 1. The use of this two-dimensional specimen greatly simplified fabrication, made possible the use of a large-scale specimen, and simplified loading and testing while preserving the key features of the joint.

To simulate combined axial load and torque, the contact surfaces between the joined components were angled at 9°30' from the longitudinal, as shown in the figure. Stress distributions through the thickness of the specimen were more easily obtained with the model scaled up to 2.5X. The model material was Photolastic PLM-4B modified for scattered light application. Model components are shown in Figure 2. A final surface finish of 8 microinches was obtained by grinding. The model was fabricated with precision so that the joint contact surface would be in full contact with the model pin inserted with a size-to-size fit. Although the polariscope system allowed photographing the model under load, the stress freezing method was used because it was mechanically simpler. The stress freezing of the model and a calibration tension specimen was carried out in a special temperature-controlled convection oven following heating and cooling cycles recommended for the given material.

The axial load was applied to the end of the model by means of a deadweight loading system (see Figure 3) which transmitted the load through a column (A) and ball (B) into the triangular loading plate (C); the spherical ball, free to roll between the loading rod and plate, ensures a vertical load at all times. Plastic

rollers (D) provide lateral support to resist any tendency toward gross bending or buckling of the specimen, particularly at the higher temperatures. A 1/8"-thick strip of silicone rubber between the aluminum loading plate and the surface of the model smoothed out localized high contact stresses and reduced surface shear stress resulting from differential thermal deformation. A scaled-down load was applied to the model. This load of 19.7 pounds was determined from the relationship

$$P_m = \frac{P_p \, E_m \, L_m \, t_m}{n \, E_p \, L_p \, t_p}$$

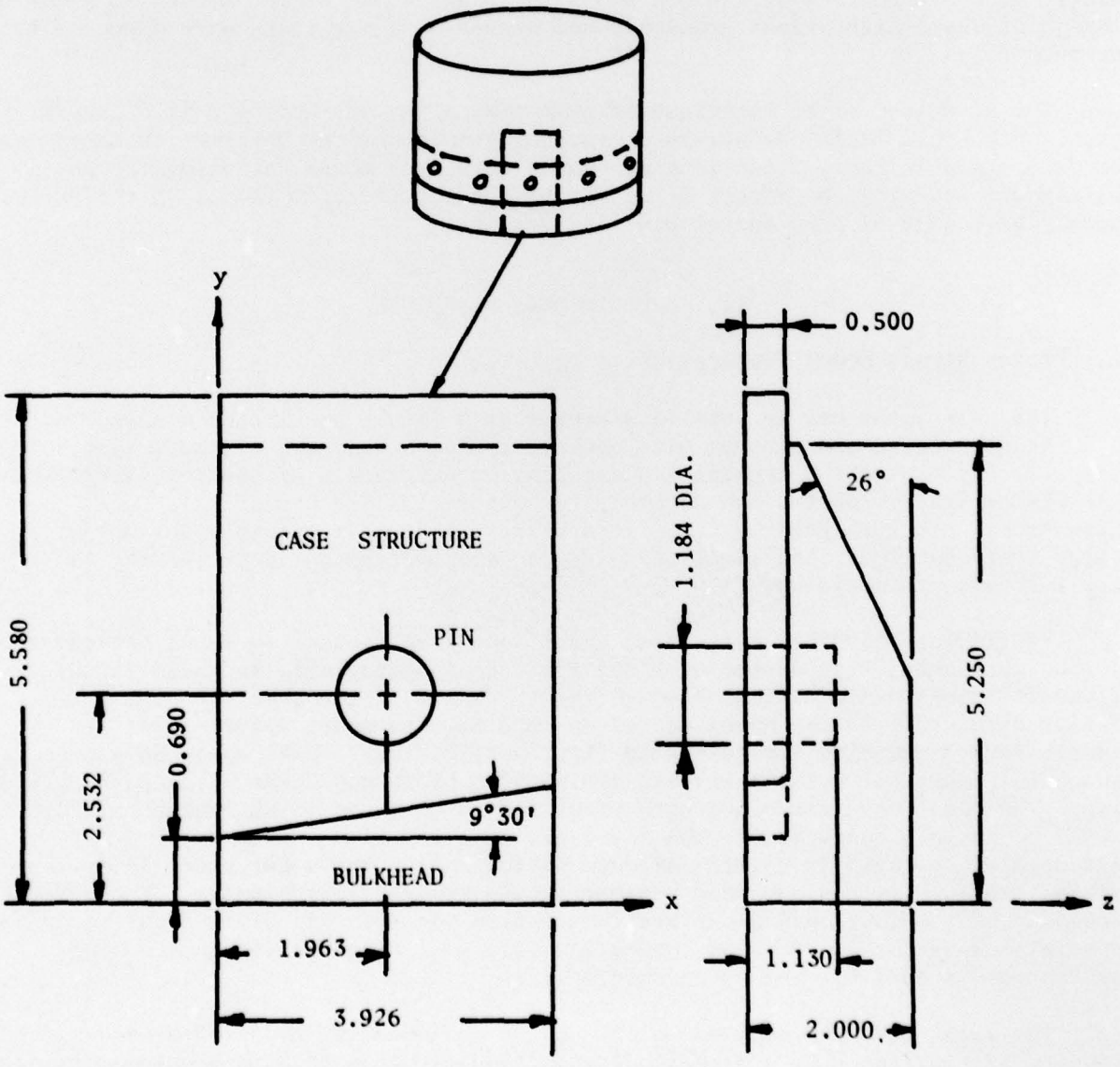

Figure 1. Two-dimensional photoelastic model of rear joint - 2.5X scale.

for which

P_m = axial load applied to model at joint (lb)

P_p = axial load applied to prototype at joint (lb)

E_m = tensile modulus of elasticity for model at the stress freezing temperature of 250 F ($lb/in.^2$)

E_p = tensile modulus of elasticity for prototype 4340 steel ($lb/in.^2$)

L_m = model width (inch)

L_p = dimension in the peripheral plane of the prototype (inch)

t_m = model thickness (inch)

t_p = prototype thickness (inch)

n = number of pins

was applied to the model.

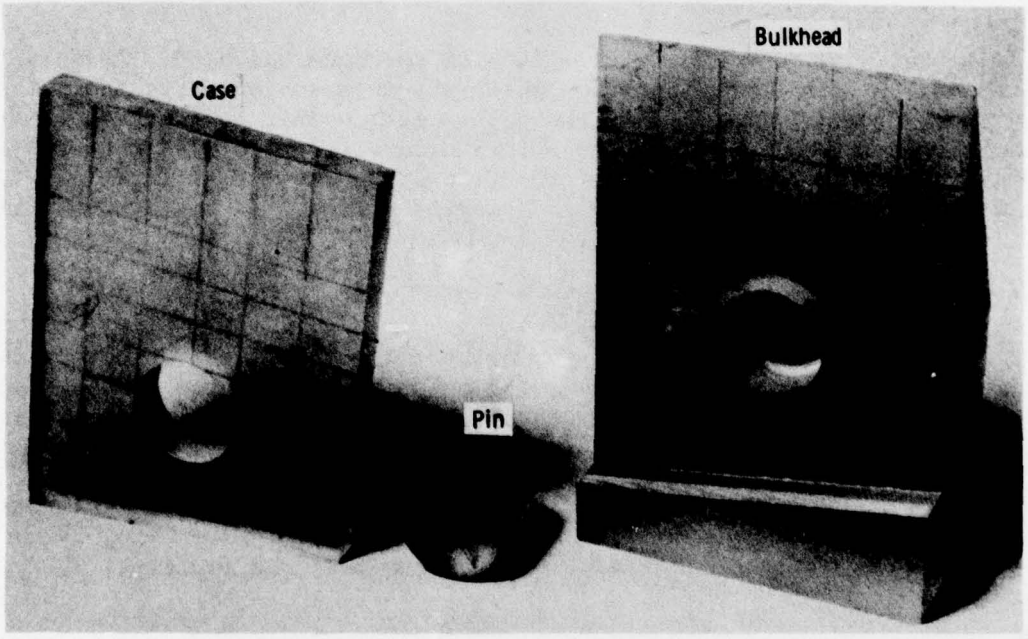

Figure 2. Machined components of the specimen.

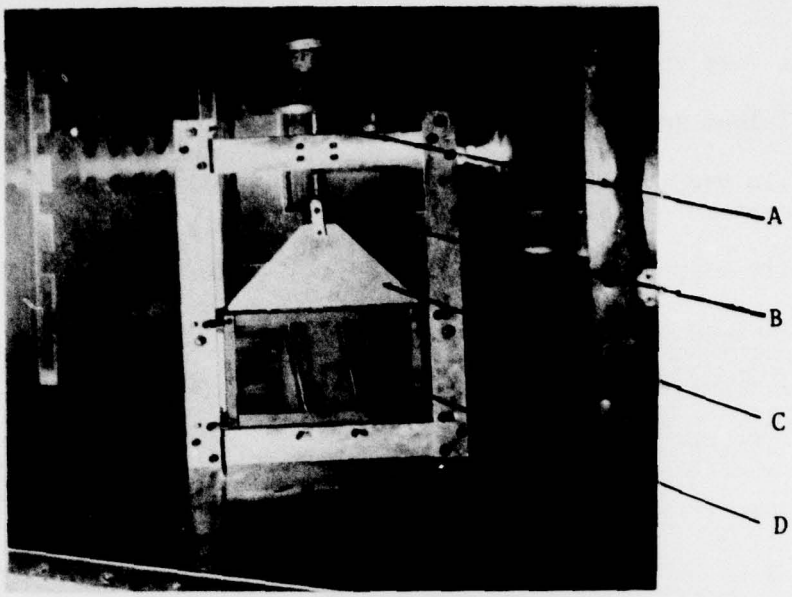

Figure 3. Assembled model in loading fixture.

B. Calibration of Model Material

To calibrate the model material a tension specimen was used. An axial load of 6.65 lb was applied to the specimen which was then subjected to the same stress-freezing cycle as that employed for the joint model. This load was chosen to produce the largest number of fringes to insure accurate determination of the fringe constant without exceeding the proportional limit of the PLM-4B material. Figure 4 shows the calibration curve based on 13 observed fringes. A calibration value of 2.16 psi/fringe/inch was obtained.

C. Scattered Light Fringe Photographs

The theory of scattered light is described in numerous references[1-4] and will not be discussed here. The stress-frozen model was mounted to the head of the polariscope and immersed in a glass-walled tank containing index-matching fluid as shown in Figure 5. The light beam from a 15-MW CW He-Ne gas laser was passed through a cylindrical lens system to expand the beam into a sheet of light 1.5 inches wide and 0.060 inch thick which entered the polariscope and model from below. The fringe patterns were recorded on 4 in. × 5 in. film using 3- to 7-minute exposures on Polaroid film 55 P/N and 3- to 6-second exposures on Polaroid film 57.

1. SRINATH, L. S., and FROCHT, M. M. *Potentialities of the Method of Scattered Light.* Proc. International Symposium of Photoelasticity, Pergamon Press, New York, 1962.
2. JESSOP, H. T. *The Scattered Light Method of Exploration of Stresses in Two- and Three-Dimensional Models.* Brit. J. Appl. Phys., v. 2, no. 9, 1951.
3. SWINSON, W. F., and BOWMAN, C. F. *Application of Scattered Light Photoelasticity to Doubly Connected Tapered Torsion Bars.* Experimental Mechanics, v. 6, no. 6, June 1966, p. 297-305.
4. SWINSON, W. F., ROLSON, W. F., and GRIFFIN, J. R. *Scattered Light Photoelastic Analysis of Epoxy Glass Structures.* U.S. Army Missile Command, Redstone Arsenal, Technical Report RL-72-16, December 1972.

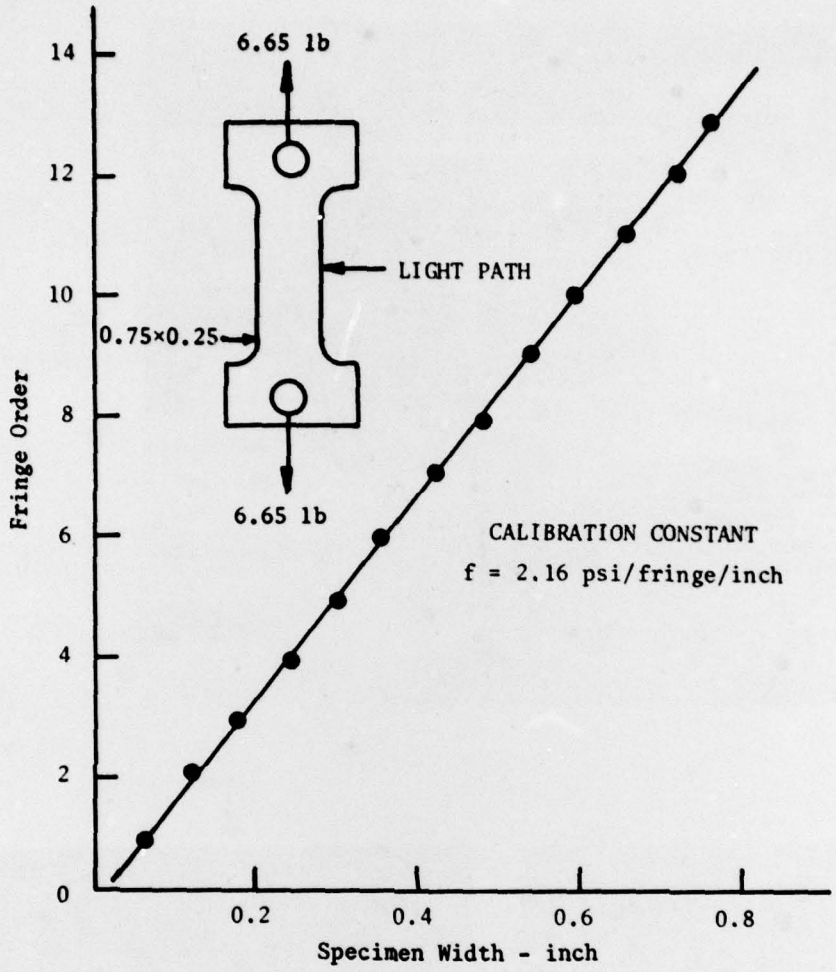

Figure 4. Calibration curve.

Laser beam axis and the glass wall of the immersion tank are fixed normal to the camera axis. The head to which the model was mounted allows rotation of the model about the laser beam axis and translation along two orthogonal axes in the horizontal plane. These motions allow the sections of the model illuminated by the laser and the angle between camera and model to be varied easily. Typical fringe patterns are shown in Figure 6.

The fringe photographs were analyzed using a microdensitometer to measure and record fringe number versus location. These data were translated into stress values by using the stress optic law $(p-q) = f(dn/ds)$, where f is the fringe constant of material, dn is an increment in the fringe order, and ds is an interval in the optical path. Distortion and obliteration of fringes occurred in some areas of the specimen because of deformation and mottling during the stress-freezing process. However, low fringe density along the y direction and light diffusion in some areas were mainly responsible for not obtaining the $\bar{\sigma}_y$ stress at some points of interest.

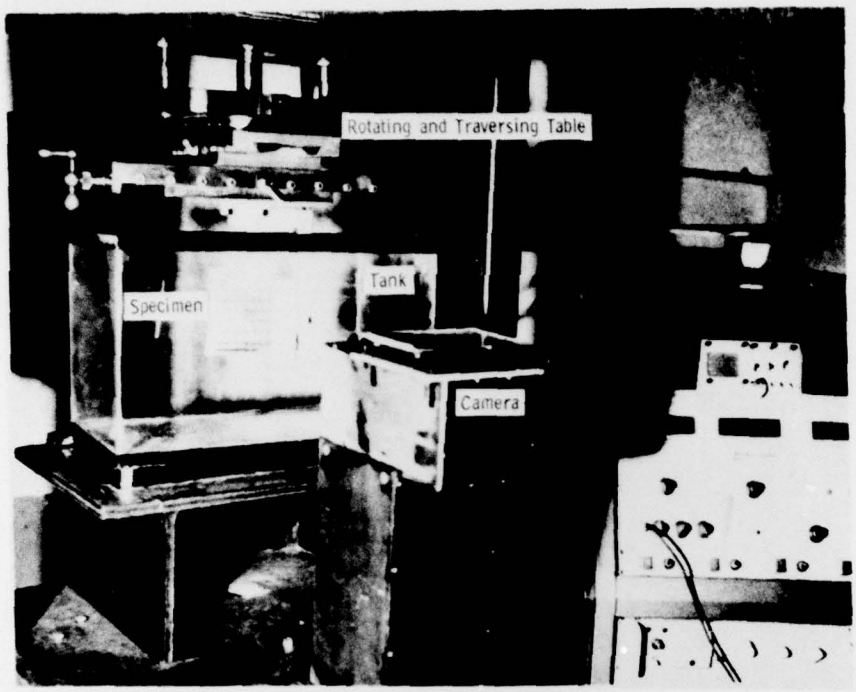

Figure 5. Test specimen mounted in polariscope.

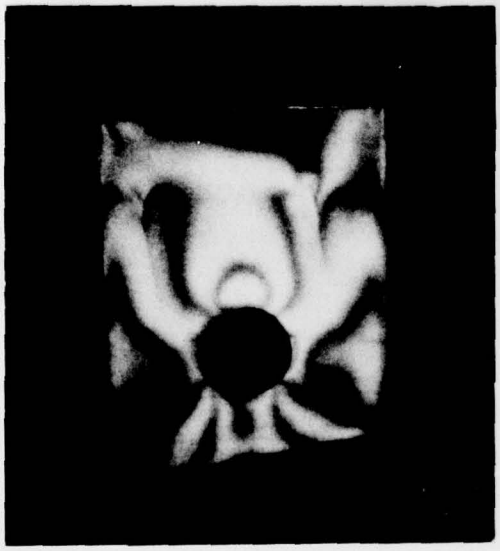

Figure 6a. Isochromatics of stress-frozen specimen.

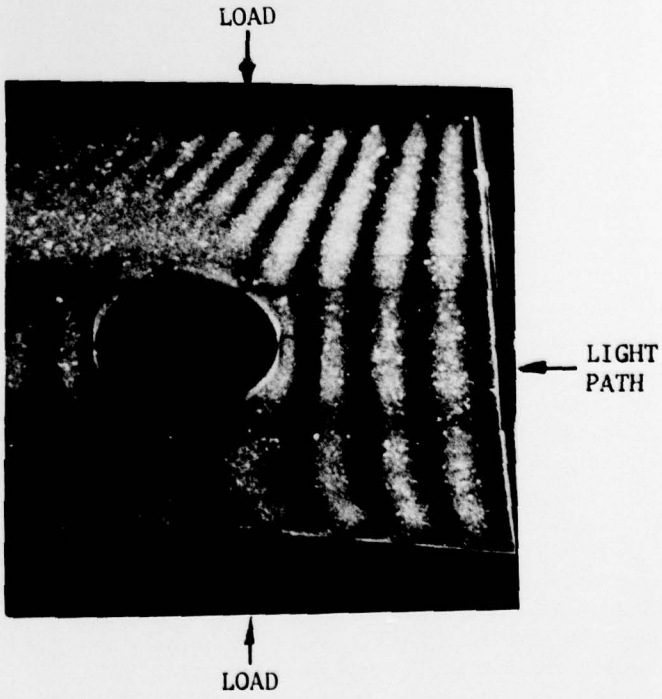

Figure 6b. Scattered light fringes of stress-frozen specimen.

Army Materials and Mechanics Research Center,
Watertown, Massachusetts 02172
SCATTERED LIGHT PHOTOELASTIC ANALYSIS OF A
PROJECTILE BULKHEAD TO STRUCTURAL CASE JOINT -
Miloslav Benicek and Jiro Adachi

AD________________

UNCLASSIFIED
UNLIMITED DISTRIBUTION

Key Words

Stress analysis
Photoelasticity
Projectiles

Technical Report AMMRC TR 79-54, October 1979, 15 pp -
illus-table, D/A Project 1X464603D663,
AMCMS Code 36525000204

Photoelastic stress analysis of the bulkhead-to-structural case pin joint of a projectile was carried out using the scattered light technique. Analysis provided three-dimensional stress distributions in critical areas of the joint including the pinhole, pin bearing surfaces, and joint bearing surfaces. Stress gradients through the wall were found to be large; however, stress concentrations were found to be moderate with a maximum value of 3.7.

Army Materials and Mechanics Research Center,
Watertown, Massachusetts 02172
SCATTERED LIGHT PHOTOELASTIC ANALYSIS OF A
PROJECTILE BULKHEAD TO STRUCTURAL CASE JOINT -
Miloslav Benicek and Jiro Adachi

AD________________

UNCLASSIFIED
UNLIMITED DISTRIBUTION

Key Words

Stress analysis
Photoelasticity
Projectiles

Technical Report AMMRC TR 79-54, October 1979, 15 pp -
illus-table, D/A Project 1X464603D663,
AMCMS Code 36525000204

Photoelastic stress analysis of the bulkhead-to-structural case pin joint of a projectile was carried out using the scattered light technique. Analysis provided three-dimensional stress distributions in critical areas of the joint including the pinhole, pin bearing surfaces, and joint bearing surfaces. Stress gradients through the wall were found to be large; however, stress concentrations were found to be moderate with a maximum value of 3.7.

Army Materials and Mechanics Research Center,
Watertown, Massachusetts 02172
SCATTERED LIGHT PHOTOELASTIC ANALYSIS OF A
PROJECTILE BULKHEAD TO STRUCTURAL CASE JOINT -
Miloslav Benicek and Jiro Adachi

AD________________

UNCLASSIFIED
UNLIMITED DISTRIBUTION

Key Words

Stress analysis
Photoelasticity
Projectiles

Technical Report AMMRC TR 79-54, October 1979, 15 pp -
illus-table, D/A Project 1X464603D663,
AMCMS Code 36525000204

Photoelastic stress analysis of the bulkhead-to-structural case pin joint of a projectile was carried out using the scattered light technique. Analysis provided three-dimensional stress distributions in critical areas of the joint including the pinhole, pin bearing surfaces, and joint bearing surfaces. Stress gradients through the wall were found to be large; however, stress concentrations were found to be moderate with a maximum value of 3.7.

Army Materials and Mechanics Research Center,
Watertown, Massachusetts 02172
SCATTERED LIGHT PHOTOELASTIC ANALYSIS OF A
PROJECTILE BULKHEAD TO STRUCTURAL CASE JOINT -
Miloslav Benicek and Jiro Adachi

AD________________

UNCLASSIFIED
UNLIMITED DISTRIBUTION

Key Words

Stress analysis
Photoelasticity
Projectiles

Technical Report AMMRC TR 79-54, October 1979, 15 pp -
illus-table, D/A Project 1X464603D663,
AMCMS Code 36525000204

Photoelastic stress analysis of the bulkhead-to-structural case pin joint of a projectile was carried out using the scattered light technique. Analysis provided three-dimensional stress distributions in critical areas of the joint including the pinhole, pin bearing surfaces, and joint bearing surfaces. Stress gradients through the wall were found to be large; however, stress concentrations were found to be moderate with a maximum value of 3.7.

Army Materials and Mechanics Research Center,
Watertown, Massachusetts 02172
SCATTERED LIGHT PHOTOELASTIC ANALYSIS OF A PROJECTILE BULKHEAD TO STRUCTURAL CASE JOINT -
Miloslav Benicek and Jiro Adachi

Technical Report AMMRC TR 79-54, October 1979, 15 pp -
illus-table, D/A Project 1X464603D663,
AMCMS Code 36525000204

AD_____

UNCLASSIFIED
UNLIMITED DISTRIBUTION

Key Words

Stress analysis
Photoelasticity
Projectiles

Photoelastic stress analysis of the bulkhead-to-structural case pin joint of a projectile was carried out using the scattered light technique. Analysis provided three-dimensional stress distributions in critical areas of the joint including the pinhole, pin bearing surfaces, and joint bearing surfaces. Stress gradients through the wall were found to be large; however, stress concentrations were found to be moderate with a maximum value of 3.7.

Army Materials and Mechanics Research Center,
Watertown, Massachusetts 02172
SCATTERED LIGHT PHOTOELASTIC ANALYSIS OF A PROJECTILE BULKHEAD TO STRUCTURAL CASE JOINT -
Miloslav Benicek and Jiro Adachi

Technical Report AMMRC TR 79-54, October 1979, 15 pp -
illus-table, D/A Project 1X464603D663,
AMCMS Code 36525000204

AD_____

UNCLASSIFIED
UNLIMITED DISTRIBUTION

Key Words

Stress analysis
Photoelasticity
Projectiles

Photoelastic stress analysis of the bulkhead-to-structural case pin joint of a projectile was carried out using the scattered light technique. Analysis provided three-dimensional stress distributions in critical areas of the joint including the pinhole, pin bearing surfaces, and joint bearing surfaces. Stress gradients through the wall were found to be large; however, stress concentrations were found to be moderate with a maximum value of 3.7.

Army Materials and Mechanics Research Center,
Watertown, Massachusetts 02172
SCATTERED LIGHT PHOTOELASTIC ANALYSIS OF A PROJECTILE BULKHEAD TO STRUCTURAL CASE JOINT -
Miloslav Benicek and Jiro Adachi

Technical Report AMMRC TR 79-54, October 1979, 15 pp -
illus-table, D/A Project 1X464603D663,
AMCMS Code 36525000204

AD_____

UNCLASSIFIED
UNLIMITED DISTRIBUTION

Key Words

Stress analysis
Photoelasticity
Projectiles

Photoelastic stress analysis of the bulkhead-to-structural case pin joint of a projectile was carried out using the scattered light technique. Analysis provided three-dimensional stress distributions in critical areas of the joint including the pinhole, pin bearing surfaces, and joint bearing surfaces. Stress gradients through the wall were found to be large; however, stress concentrations were found to be moderate with a maximum value of 3.7.

Army Materials and Mechanics Research Center,
Watertown, Massachusetts 02172
SCATTERED LIGHT PHOTOELASTIC ANALYSIS OF A PROJECTILE BULKHEAD TO STRUCTURAL CASE JOINT -
Miloslav Benicek and Jiro Adachi

Technical Report AMMRC TR 79-54, October 1979, 15 pp -
illus-table, D/A Project 1X464603D663,
AMCMS Code 36525000204

AD_____

UNCLASSIFIED
UNLIMITED DISTRIBUTION

Key Words

Stress analysis
Photoelasticity
Projectiles

Photoelastic stress analysis of the bulkhead-to-structural case pin joint of a projectile was carried out using the scattered light technique. Analysis provided three-dimensional stress distributions in critical areas of the joint including the pinhole, pin bearing surfaces, and joint bearing surfaces. Stress gradients through the wall were found to be large; however, stress concentrations were found to be moderate with a maximum value of 3.7.

III. EXPERIMENTAL RESULTS

A. General

Stress results obtained are shown in Figures 7 through 10 and in Table 1. These results were obtained using scattered light photoelasticity in a two-dimensional plane-stress problem. Since in this case only in-plane normal stress perpendicular to the direction of light propagation contributes to the fringe formation, values of this stress are obtained directly and no stress separation is required. Stress variations through the specimen thickness were obtained by traversing the light along the z direction. Only the information of significant interest to the current problem are presented here. The primary interest was phenomenological. It was necessary to obtain an insight into how the pin behaved under the axial setback loads and the effect of this behavior on the distribution of stresses in the joint region. Of further interest and of direct and immediate relevance to the problem was the magnitude and location of high stresses and strains.

Table 1. DISTRIBUTION OF $\bar{\sigma}_y$ STRESS THROUGH SPECIMEN THICKNESS AND ALONG LINE mn

x \ z	$\bar{\sigma}_y$ (COMPRESSION)						
	0.000"	0.060"	0.013"	0.250"	0.350"	0.450"	0.500"
0	0.89	0.87	0.83	0.55	0.67	0.94	1.10
0.25	.91	.89	.85	.55	.67	.92	1.08
0.50	.95	.92	.81	.72	.72	.96	1.12
0.75	.83	.82	.81	.75	.75	1.20	1.45
1.00	.89	.87	.81	.72	.81	1.20	1.50
1.25	.93	.89	.81	.77	.87	1.60	1.90
1.50	.40	.60	.85	.72	1.10	1.80	2.30
1.75	.48	.58	.77	1.10	1.70	2.40	2.80
1.96	.45	.55	.76	1.30	1.90	3.00	3.70

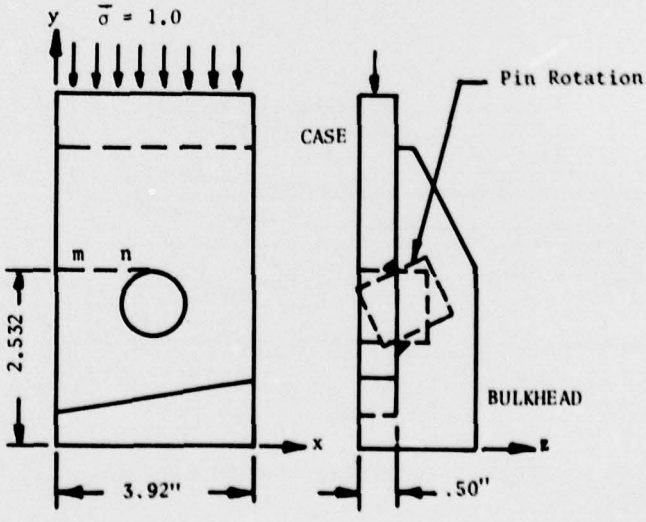

In presenting the data, the stresses σ have been converted into dimensionless form $\bar{\sigma}$ by dividing the actual stresses by the average nominal stress determined at the horizontal cross section 1.5 inches above the top of the pinhole. The stresses reported are those caused by the simulated axial and torsional loads only and do not include the prestress effect of initial interference between pin and pinhole. Also, since the stress distributions and magnitudes are almost the same on either side of the vertical centerline of the pin, only one side is shown on most of the figures and in Table 1. All dimensions shown refer to the model, which is 2.5 times the size of the prototype.

B. Pin Behavior and Effect

1. The three-dimensional distributions of the axial stresses $\bar{\sigma}_y$ on the plane through the top of the pin, Figure 7, shows the effect of the pin on stresses, which without the pin would be fairly uniform. The steep stress gradient along the top of the pin (x = 1.96, z = 0 to 0.50) is clearly the effect of pivoting of the pin as it transfers load into the bulkhead as shown schematically in the figure accompanying Table 1.

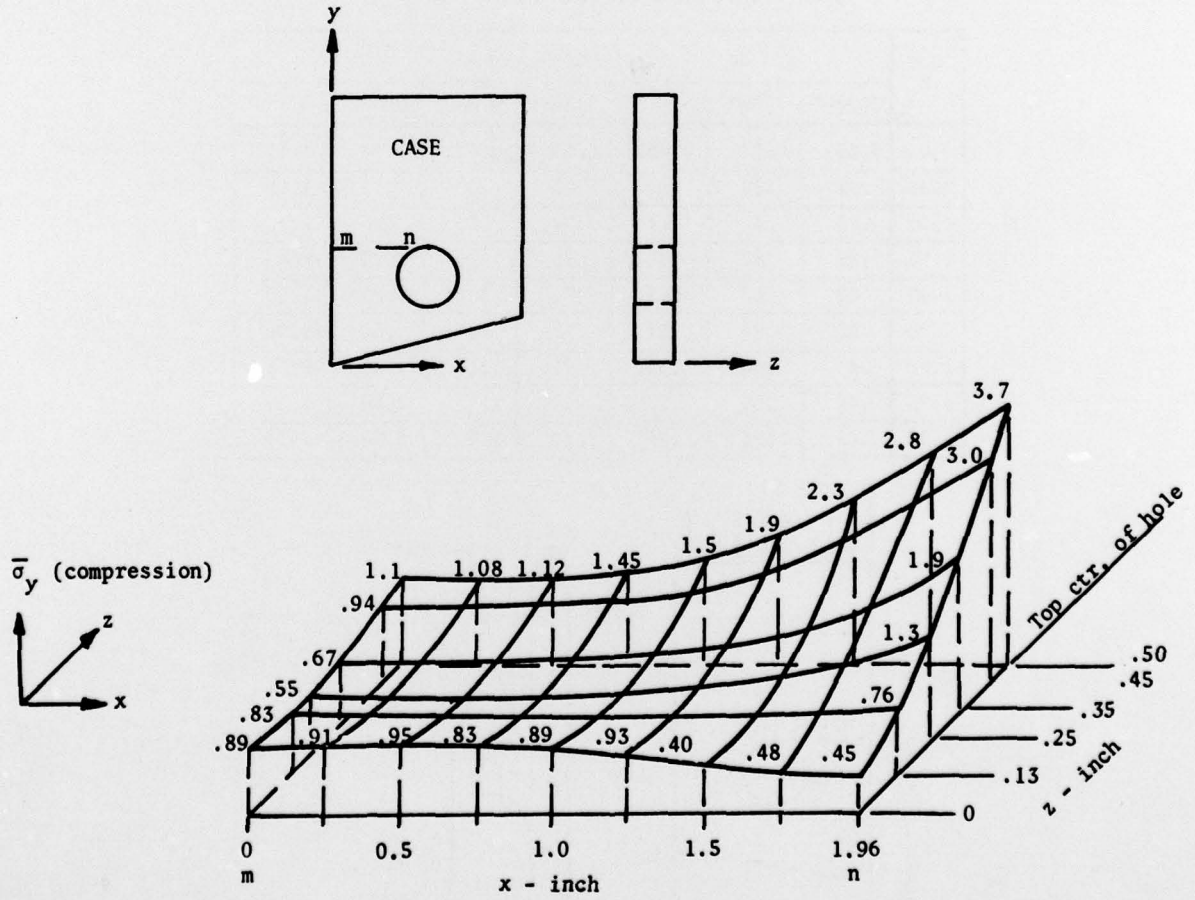

Figure 7. $\bar{\sigma}_y$ stress contours along line mn.

Since the pin in this case is short, with a length-to-diameter ratio of about one, the movement of the pin is a combination primarily of shear deformation and rigid body rotation or pivoting. Of additional phenomenological interest is the fact that contact is maintained between pin and component along the full length of the pin as evidenced by the non-zero normal stress at all points along the top of the pin. With much larger length-to-diameter ratios, i.e., more flexible pins, the effect of bending deformation would become important. However, for the usual pin configurations used, length-to-diameter ratios of up to two or three, the behavior is probably as demonstrated here.

Figure 8 shows the $\bar{\sigma}_y$ stress distribution on the horizontal plane through the center of the pin. The greatly reduced peak stress levels are partially a reflection of the reduction of the total load in the section as the result of the transfer of load through the pin into the other components (the bulkhead).

The distribution in Figure 8 is much more uniform than that in Figure 7, which is probable indication that the effect of pivoting of the pin and the resulting highly concentrated stress effects on the top of the pin dissipate rapidly along the boundary of the pin from the top to the side.

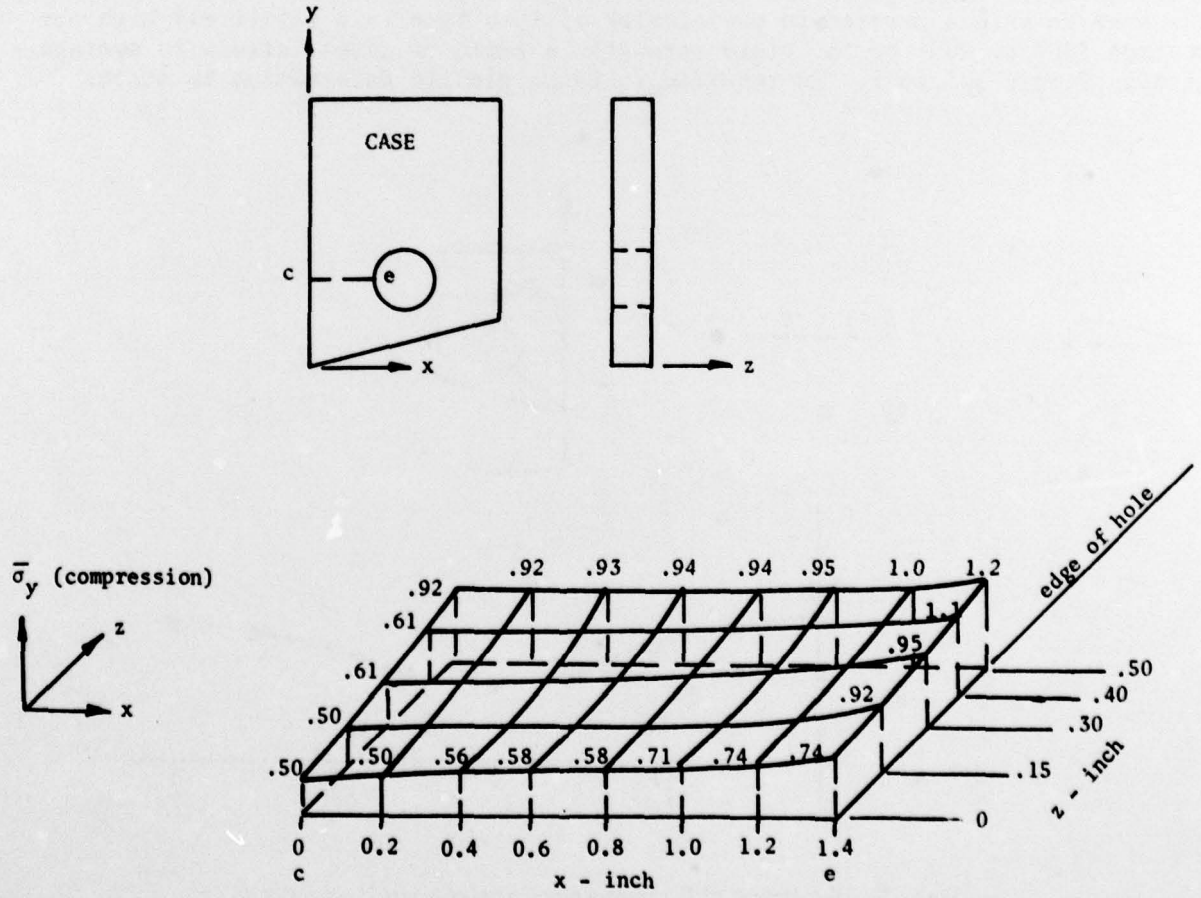

Figure 8. $\bar{\sigma}_y$ stress contours along line ce.

2. The transfer of load through the pin into the bulkhead has the effect of reducing the contact stresses on the joint interface directly below the pin as shown in Figure 9. Integration of the stresses in Figure 8 over the cross-sectional area reveals that one-third of the total load is transferred through the pin into the bulkhead. Redistribution of the uneven stress distribution caused by this transfer has not occurred, probably since the edge distance of the pin from joint interface is very short.

3. Figure 10 shows typical values of the actual-to-average axial stress ratios $\bar{\sigma}_y$ within the case structure. The ratios along the upper portions of the case are all 1.0, indicating that the influence of the pin discontinuity does not extend beyond about one pin diameter above the pin.

The symmetry of the stress magnitudes about the vertical centerline of the pin shows that the effect of the sloping bottom (or the torsion load) on the symmetry is not significant.

C. Stress and Strain Magnitude

The complicated interaction of the pin with the joined components makes the seriousness of the high stress concentration factors difficult to assess. Since the average stress carried in projectiles of this type is a relatively high percentage (85% to 90%) of the yield strength, a ratio of actual stress to average stress of only 1.1 to 1.2 is required to cause plastic deformation to start.

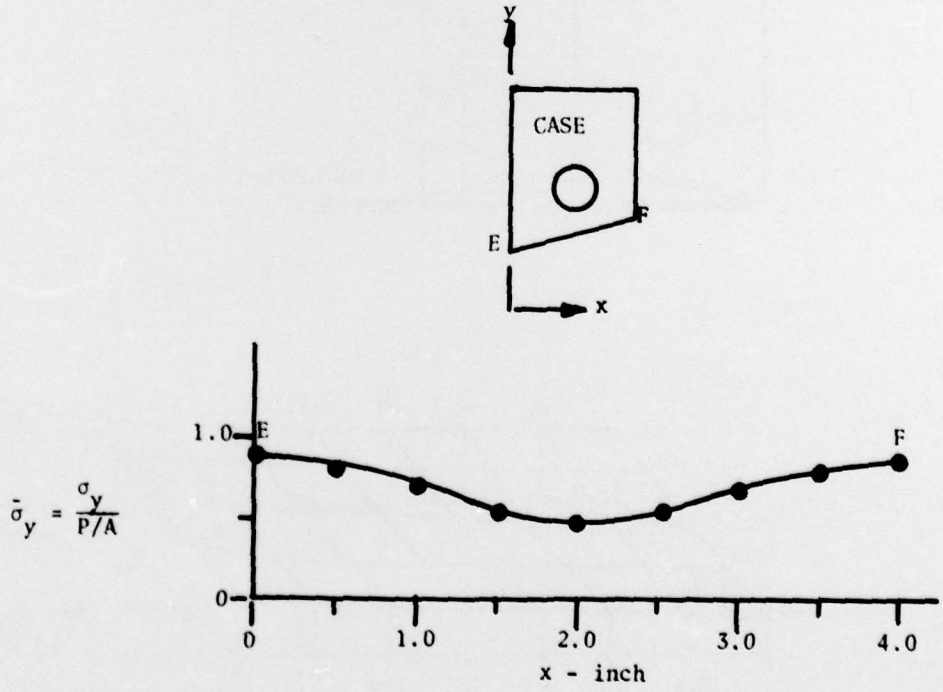

Figure 9. Distribution of $\bar{\sigma}_y$ stress along length of joint EF (z = 0.35").

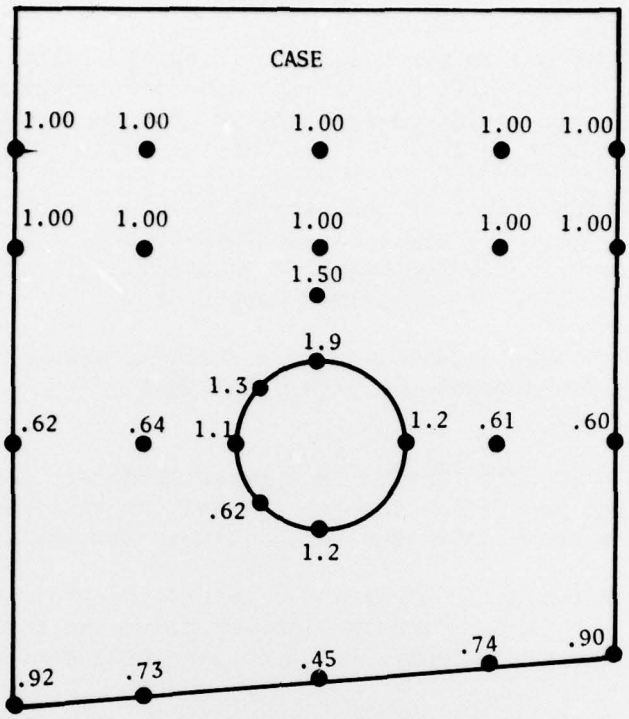

Figure 10. Values of $\bar{\sigma}_y$ stress at various locations (z = 0.35").

Since the actual-to-average stress ratios in the joint reach magnitudes well above 1.2 and up to 3.7, the occurrence of plastic strain ranging up to about 2% appears possible under design loading conditions. The actual magnitudes and locations of plastic strain cannot be determined without a three-dimensional elastic-plastic analysis.

The seriousness of such behavior depends on the ability of the material to undergo such large strains without deterioration of its ability to carry other subsequent loads. Tough, ductile materials can safely absorb larger degrees of plastic strain than less ductile, less tough materials.

If the average effective stress over the pin periphery is less than the yield strength of the material, gross yielding over the entire pin contact area would not occur although extensive redistribution of stress and load will occur. If the average effective stress exceeds the yield strength, significant plastic yielding over the entire pin could occur, with excessively high plastic deformation accompanied by serious deterioration of material properties, including cracking. This deterioration would reduce the strength of the structure against subsequent forces in other directions and could possibly lead to catastropic failure.

IV. CONCLUSIONS

Various conclusions can be drawn from the findings relative to the completeness of the study and the significance of the findings to the current problem, and to pin joint design for advanced projectiles or other applications in general. The more urgent conclusions follow.

1. The complicating effect of the pins in a joint leads to high stress gradients and high stress magnitudes which can in turn result in plastic deformation of a magnitude which, depending on the material capabilities, can seriously reduce the structural survivability of the joined components.

2. Scattered light photoelasticity is a straightforward and sufficiently accurate method for three-dimensional stress analysis of complex structural configurations.

3. For photographing the fringes in a given plane section of a specimen, the technique of moving the test model through a fixed concentrated laser beam is more effective than using a broad thin beam which illuminates the entire section.

4. Additional photoelastic studies are needed to obtain data on the elastic stress distributions for various combinations of pin joint configurations to provide a broader basis for preliminary design of pin joint configurations and dimensions.

5. There remains to be demonstrated the feasibility and economy of superimposing applied loads on a frozen stress system, for example, the effect of different pin interference on the overall stress values in a joint.

6. There remains a need for an effective method (either mathematical or experimental) for three-dimensional elastic-plastic analysis of complex joint geometries.

DISTRIBUTION LIST

No. of Copies	To
1	Office of the Under Secretary of Defense for Research and Engineering, The Pentagon, Washington, D.C. 20301
12	Commander, Defense Documentation Center, Cameron Station, Building 5, 5010 Duke Street, Alexandria, Virginia 22314
1	Metals and Ceramics Information Center, Battelle Columbus Laboratories, 505 King Avenue, Columbus, Ohio 43201
	Deputy Chief of Staff, Research, Development, and Acquisition, Headquarters Department of the Army, Washington, D. C. 20310
1	ATTN: DAMA-ARZ
	Commander, Army Research Office, P. O. Box 12211, Research Triangle Park, North Carolina 27709
1	ATTN: Information Processing Office
1	Dr. F. W. Schmiedeshoff
	Commander, U. S. Army Materiel Development and Readiness Command, 5001 Eisenhower Avenue, Alexandria, Virginia 22333
1	ATTN: DRCLDC, Mr. R. Zentner
	Commander, U. S. Army Materiel Systems Analysis Activity, Aberdeen Proving Ground, Maryland 21005
1	ATTN: DRXSY-MP, H. Cohen
	Commander, U. S. Army Electronics Research and Development Command, Fort Monmouth, New Jersey 07703
1	ATTN: DELSD-L
1	DELSD-E
	Commander, U. S. Army Missile Command, Redstone Arsenal, Alabama 35809
1	ATTN: DRSMI-RKP, J. Wright, Bldg. 7544
	Commander, U. S. Army Natick Research and Development Command, Natick, Massachusetts 01760
1	ATTN: Technical Library
1	Dr. E. W. Ross
1	DRDNA-UE, Dr. L. A. McClaine
	Commander, U. S. Army Satellite Communications Agency, Fort Monmouth, New Jersey 07703
1	ATTN: Technical Document Center
	Commander, U. S. Army Tank-Automotive Research and Development Command, Warren, Michigan 48090
1	ATTN: DRDTA-RKA
1	DRDTA-UL, Technical Library
	Commander, U. S. Army Armament Research and Development Command, Dover, New Jersey 07801
2	ATTN: Technical Library
1	DRDAR-SCM, J. D. Corrie
1	Dr. J. Fraiser
1	Mr. Harry E. Pebly, Jr., PLASTEC, Director
	Commander, White Sands Missile Range, New Mexico 88002
1	ATTN: STEWS-WS-VT
	Commander, U. S. Army Armament Research and Development Command, Aberdeen Proving Ground, Maryland 21010
1	ATTN: DRDAR-QAC-E
	Commander, U. S. Army Ballistic Research Laboratory, Aberdeen Proving Ground, Maryland 21005
1	ATTN: Dr. R. Vitali
1	Dr. W. Gillich
1	Mr. A. Elder
1	DRDAR-TSB-S (STINFO)
	Commander, Harry Diamond Laboratories, 2800 Powder Mill Road, Adelphi, Maryland 20783
1	ATTN: Technical Information Office
	Commander, Picatinny Arsenal, Dover, New Jersey 07801
1	ATTN: Mr. A. M. Anzalone, Bldg. 3401
1	Mr. J. Pearson
1	G. Randers-Pehrson
1	SARPA-RT-S
	Commander, Redstone Scientific Information Center, U. S. Army Missile Command, Redstone Arsenal, Alabama 35809
1	ATTN: DRSMI-TB
	Commander, Watervliet Arsenal, Watervliet, New York 12189
1	ATTN: Mr. D. P. Kendall
1	Mr. J. F. Throop
	Commander, U. S. Army Foreign Science and Technology Center, 220 7th Street, N. E., Charlottesville, Virginia 22901
1	ATTN: Mr. Marley, Military Tech
	Chief, Benet Weapons Laboratory, LCWSL, USA ARRADCOM, Watervliet Arsenal, Watervliet, New York 12189
1	ATTN: DRDAR-LCB-TL
	Director, Eustis Directorate, U. S. Army Air Mobility Research and Development Laboratory, Fort Eustis, Virginia 23604
1	ATTN: Mr. J. Robinson, DAVDL-E-MOS (AVRADCOM)
	U. S. Army Aviation Training Library, Fort Rucker, Alabama 36360
1	ATTN: Building 5906-5907
	Commander, U. S. Army Agency for Aviation Safety, Fort Rucker, Alabama 36362
1	ATTN: Librarian, Bldg. 4905
	Commander, USACDC Air Defense Agency, Fort Bliss, Texas 79916
1	ATTN: Technical Library
	Commander, U. S. Army Engineer School, Fort Belvoir, Virginia 22060
1	ATTN: Library
	Commander, U. S. Army Engineer Waterways Experiment Station, Vicksburg, Mississippi 39180
1	ATTN: Research Center Library
	Commander, Naval Air Engineering Center, Lakehurst, New Jersey 08733
1	ATTN: Technical Library, Code 1115
	Director, Structural Mechanics Research, Office of Naval Research, 800 North Quincy Street, Arlington, Virginia 22203
1	ATTN: Dr. N. Perrone
	David Taylor Naval Ship Research and Development Laboratory, Annapolis, Maryland 21402
1	ATTN: Dr. H. P. Chu
	Naval Research Laboratory, Washington, D.C. 20375
1	ATTN: C. D. Beachem, Head, Adv. Mat'ls Tech Br. (Code 6310)
1	Dr. J. M. Krafft - Code 8430
1	Dr. Jim C. I. Chang
	Chief of Naval Research, Arlington, Virginia 22217
1	ATTN: Code 471
	Naval Weapons Laboratory, Washington, D.C. 20390
1	ATTN: H. W. Romine, Mail Stop 103
1	Ship Research Committee, Maritime Transportation Research Board, National Research Council, 2101 Constitution Avenue, N. W., Washington, D.C. 20418
	Air Force Materials Laboratory, Wright-Patterson Air Force Base, Ohio 45433
1	ATTN: AFML (MXE), E. Morrissey
1	AFML (LC)
1	AFML (LLP), D. M. Forney, Jr.
1	AFML (MBC), Mr. Stanley Schulman
	Air Force Flight Dynamics Laboratory, Wright-Patterson Air Force Base, Ohio 45433
1	ATTN: AFFDL (FBS), C. Wallace
1	AFFDL (FBE), G. D. Sendeckyj

No. of Copies	To
	National Aeronautics and Space Administration, Washington, D.C. 20546
1	ATTN: Mr. B. G. Achhammer
1	Mr. G. C. Deutsch - Code RW
	National Aeronautics and Space Administration, Marshall Space Flight Center, Huntsville, Alabama 35812
1	ATTN: R. J. Schwinghamer, EH01, Dir., M&P Lab
1	Mr. W. A. Wilson, EH41, Bldg. 4612
	National Aeronautics and Space Administration, Langley Research Center, Hampton, Virginia 23665
1	ATTN: Mr. H. F. Hardrath, Mail Stop 188M
1	Mr. R. Foye, Mail Stop 188A
1	Dr. R. J. Hayduk, Mail Stop 243
	National Aeronautics and Space Administration, Lewis Research Center, 21000 Brookpark Road, Cleveland, Ohio 44135
1	ATTN: Mr. R. F. Lark, Mail Stop 49-3
	Lockheed-Georgia Company, 86 South Cobb Drive, Marietta, Georgia 30063
1	ATTN: Materials & Processes Eng. Dept. 71-11, Zone 54
	National Bureau of Standards, U. S. Department of Commerce, Washington, D.C. 20234
1	ATTN: Mr. J. A. Bennett
1	Mechanical Properties Data Center, Belfour Stulen Inc., 13917 W. Bay Shore Drive, Traverse City, Michigan 49684
1	Dr. J. Charles Grosskreutz, Asst. Dir. for Research, Solar Energy Research Institute, 1536 Cole Boulevard, Golden, Colorado 80401
	Southwest Research Institute, 8500 Culebra Road, San Antonio, Texas 78284
1	ATTN: Dr. P. Francis
1	Dr. W. Baker
1	Dr. E. A. Steigerwald, TRW Metals Division, P. O. Box 250, Minerva, Ohio 44657
1	Dr. George R. Irwin, Department of Mechanical Engineering, University of Maryland, College Park, Maryland 20742
	Battelle Columbus Laboratories, 505 King Avenue, Columbus, Ohio 43201
1	ATTN: Mr. J. Campbell
	General Electric Company, Knolls Atomic Power Laboratory, P. O. Box 1072, Schenectady, New York 12301
1	ATTN: Mr. F. J. Mehringer
1	Dr. L. F. Coffin, Room 1C41-K1, Corp. R&D, General Electric Company, P. O. Box 8, Schenectady, New York 12301
	United States Steel Corporation, Monroeville, Pennsylvania 15146
1	ATTN: Dr. A. K. Shoemaker, Research Laboratory, Mail Stop 78
	Westinghouse Electric Company, Bettis Atomic Power Laboratory, P. O. Box 79, West Mifflin, Pennsylvania 15122
1	ATTN: Mr. R. G. Hoppe, Manager
	Westinghouse Research and Development Center, 1310 Beulah Road, Pittsburgh, Pennsylvania 15235
1	ATTN: Mr. E. T. Wessel
1	Mr. M. J. Manjoine
	Brown University, Providence, Rhode Island 02912
1	ATTN: Prof. W. N. Findley, Division of Engineering, Box D
	Carnegie-Mellon University, Department of Mechanical Engineering, Schenley Park, Pittsburgh, Pennsylvania 15213
1	ATTN: Dr. J. L. Swedlow

No. of Copies	To
1	Prof. J. D. Lubahn, Colorado School of Mines, Golden, Colorado 80401
1	Prof. J. Dvorak, Civil Engineering Department, Duke University, Durham, North Carolina 27706
	George Washington University, School of Engineering and Applied Sciences, Washington, D.C. 20052
1	ATTN: Dr. H. Liebowitz
	Terra Tek, University Research Park, 420 Wakara Way, Salt Lake City, Utah 84108
1	ATTN: Dr. A. Jones
1	Librarian, Material Sciences Corporation, Blue Bell Office Campus, Merion Towle House, Blue Bell, Pennsylvania 19422
	Massachusetts Institute of Technology, Cambridge, Massachusetts 02139
1	ATTN: Prof. F. A. McClintock, Room 1-304
1	Prof. T. H. H. Pian, Department of Aeronautics and Astronautics
1	Prof. A. S. Argon, Room 1-306
1	Prof. J. N. Rossettos, Department of Mechanical Engineering, Northeastern University, Boston Massachusetts 02115
1	Prof. R. Greif, Department of Mechanical Engineering, Tufts University, Medford, Massachusetts 02155
1	Dr. D. E. Johnson, AVCO Systems Division, Wilmington, Massachusetts 01887
	University of Delaware, Department of Aerospace and Mechanical Engineering, Newark, Delaware 19711
1	ATTN: Prof. B. Pipes
1	Prof. J. Vinson
	Syracuse University, Department of Chemical Engineering and Metallurgy, 409 Link Hall, Syracuse, New York 13210
1	ATTN: Mr. H. W. Liu
1	Prof. W. Goldsmith, Department of Mechanical Engineering, University of California, Berkeley, California 94720
1	Prof. A. J. McEvily, Metallurgy Department U-136, University of Connecticut, Storrs, Connecticut 06268
1	Prof. D. Drucker, Dean of School of Engineering, University of Illinois, Champaign, Illinois 61820
1	Prof. R. I. Stephens, Materials Engineering Division, University of Iowa, Iowa City, Iowa 52242
1	Prof. D. K. Felbeck, Department of Mechanical Engineering, University of Michigan, 2046 East Engineering, Ann Arbor, Michigan 48109
1	Dr. M. L. Williams, Dean of Engineering, 240 Benedum Hall, University of Pittsburgh, Pittsburgh, Pennsylvania 15260
1	Prof. A. Kobayashi, Department of Mechanical Engineering, FU-10, University of Washington, Seattle, Washington 98195
	State University of New York at Stony Brook, Stony Brook, New York 11790
1	ATTN: Prof. Fu-Pen Chiang, Department of Mechanics
	Denver Research Institute, 2390 South University Boulevard, Denver, Colorado 80210
1	ATTN: Dr. R. Recht
1	Dr. Robert S. Shane, Shane Associates, Inc., 7821 Carrleigh Parkway, Springfield, Virginia 22152
	Director, Army Materials and Mechanics Research Center, Watertown, Massachusetts 02172
2	ATTN: DRXMR-PL
1	DRXMR-WD
2	Authors